Physics Letters B 744 (2015) 1–6

Contents lists available at ScienceDirect

Physics Letters B

www.elsevier.com/locate/physletb

Strong decays of vector mesons to pseudoscalar mesons in the relativistic quark model

D. Ebert [a], R.N. Faustov [b], V.O. Galkin [b,*]

[a] Institut für Physik, Humboldt–Universität zu Berlin, Newtonstrasse 15, D-12489 Berlin, Germany
[b] Dorodnicyn Computing Centre, Russian Academy of Sciences, Vavilov Street 40, 119333 Moscow, Russia

ARTICLE INFO

Article history:
Received 17 December 2014
Received in revised form 5 March 2015
Accepted 10 March 2015
Available online 14 March 2015
Editor: J.-P. Blaizot

ABSTRACT

Strong decays of vector ($^3S_1$) mesons to the pair of pseudoscalar ($^1S_0$) mesons are considered in the framework of the microscopic decay mechanism and the relativistic quark model based on the quasipotential approach. The quark–antiquark potential, which was previously used for the successful description of meson spectroscopy and electroweak decays, is employed as the source of the $q\bar{q}$ pair creation. The relativistic structure of the decay matrix element, relativistic contributions and boosts of the meson wave functions are comprehensively taken into account. The calculated rates of strong decays of light, heavy-light mesons and heavy quarkonia agree well with available experimental data.

1. Introduction

At present a large set of experimental data is available on light and heavy mesons which is constantly extending [1]. Recently, the most dramatic progress has been achieved in the heavy meson sector. As a result, in the last years many new charmonium states and new bottomonium states have been discovered [2]. The number of the open-flavor (charmed D and bottom B) meson states is also constantly increasing. Some of the new states are the long-awaited ones, expected within the constituent quark model many years ago, while some others, with masses higher than the thresholds of the open charm and bottom production, have narrow widths and unexpected decay properties [1,2]. Similar exotic states are known in the light meson sector. There are theoretical indications [2] that some of these states could be the first manifestation of the existence of exotic hadrons (tetraquarks, molecules, hybrids etc.), which are predicted to exist within quantum chromodynamics (QCD). In order to explore such entities, a comprehensive understanding of the meson spectroscopy and decays up to rather high orbital and radial excitations is required.

Thus, one of the important issues is the study of strong meson decays. Such decays are the main channels for mesons with masses above open flavor production thresholds. They are investigated already for many years. Nevertheless, strong decays still constitute a rather poorly understood area of hadronic physics in view of their complex nonperturbative dynamics, which has not yet been deduced directly from QCD.

Several phenomenological models of open-flavor strong decays have been proposed and described in the literature. Some of them are based on effective chiral meson Lagrangians derived from the Nambu–Jona-Lasinio quark model (see e.g. [3] and the references therein), which express decay amplitudes through quark loop integrals with quark propagators between initial and final meson vertices. However, such considerations of strong decays do not account for quark confinement and momentum-dependence of vertices. In particular, vertices are considered to be point-like and, as a result, quark loop integrals diverge. Thus, the introduction of some phenomenological cutoff parameter is necessary.

The other group of approaches are based on different types of quark pair creation models. They differ in the production mechanism of a light quark pair from the QCD vacuum. The phenomenological $^3S_1$ model [4] considers the corresponding quark–antiquark pair to be produced in the vector state. However, this appears to disagree with experiment and is thus ruled out [5].

The most popular approach to strong meson decays is based on the phenomenological $^3P_0$ model (see [2,5,6] and the references therein). This model assumes that the quark–antiquark pair is created with the vacuum quantum numbers, $J^{PC} = 0^{++}$. It gives for most decays results in fairly good agreement with experimental data. The important features of the model are its simplicity and necessity to introduce only one additional parameter, the strength of the decay interaction, in order to describe various strong decays. This parameter is considered as a free constant and is fitted to the

* Corresponding author.
E-mail address: galkin@ccas.ru (V.O. Galkin).

http://dx.doi.org/10.1016/j.physletb.2015.03.019

data. It is generally believed that the pair production strength parameter is roughly flavor independent, but recent studies, involving a global fit of the experimental data, indicate that it can be scale dependent [7]. However, this model does not clarify the fundamental mechanism of pair creation. It has an explicitly nonrelativistic character with meson wave functions modeled by simple Gaussian functions. All this makes it very difficult to improve the model.

Another approach, closely related to the $^3P_0$ model, is the flux-tube breaking model [8]. It also assumes that a quark–antiquark pair is created with the vacuum quantum numbers, but it additionally includes the overlaps of the flux-tube of the initial meson with those of the two final mesons. Therefore, the resulting calculations are more complicated, but lead to predictions close to the results of the $^3P_0$ model.

In the microscopic decay model [9], which is more closely related to QCD, the pair creation originates from the current–current interactions due to the potential binding quarks in mesons, which is usually assumed to be the sum of the scalar confining interaction and the one gluon exchange. It generalizes the above approaches, which can be obtained as its special limiting cases. Thus, the $^3P_0$ model results are reproduced with the constant scalar interaction. In contrast to the $^3P_0$ model, the strong decay rates are completely determined by the meson wave functions, quark masses and interaction parameters. At present, most calculations are done in the nonrelativistic constituent quark model with spherical harmonic oscillator wave functions.

In Ref. [10] a model of strong decays has been proposed, where the pair creation occurs due to the string breaking. The basic interaction in this model is the scalar color-singlet confining potential acting between the light quark and heavy antiquark. It is flavor independent and nonlocal for the zero mass light quark pair, turning to the linearly rising confining potential for a long breaking string. There is a direct correspondence between the string breaking model and the microscopic decay model with the scalar potential, but the former uses a relativistic formalism for light quarks with vanishing current masses.

In this paper we propose a relativistic approach for the calculation of strong decays of mesons in the framework of the previously developed relativistic quark model [11,12] based on the quasipotential approach. For this purpose, the microscopic decay model is extended to include relativistic effects into decay matrix elements, relativistic corrections and boosts of the meson wave functions. The QCD-motivated quark–antiquark interaction potential, which was previously found to reproduce well mass spectra and electroweak decays of mesons, is used for the description of the pair creation mechanism. The resulting relativistic calculations are rather complicated. As a first step, we consider the simplest case, where only S-wave mesons are involved. This significantly simplifies the angular structure of decay matrix elements. The comparison of the obtained results with the available experimental data for the decays of vector ($^3S_1$) mesons to a pair of pseudoscalar ($^1S_0$) mesons provides a test of our approach.

2. Relativistic quark model

For the following calculations we use the relativistic quark model based on the quasipotential approach and quantum chromodynamics (QCD). Mesons are considered as the bound states of constituent quarks which are described by the single-time wave functions satisfying the three-dimensional relativistically invariant Schrödinger-like equation with the QCD-motivated interquark potential [11]

$$\left(\frac{b^2(M)}{2\mu_R}-\frac{\mathbf{p}^2}{2\mu_R}\right)\Psi_M(\mathbf{p})=\int\frac{d^3q}{(2\pi)^3}V(\mathbf{p},\mathbf{q};M)\Psi_M(\mathbf{q}), \tag{1}$$

with the relativistic reduced mass defined by

$$\mu_R=\frac{M^4-(m_1^2-m_2^2)^2}{4M^3}, \tag{2}$$

where M is the meson mass, $m_{1,2}$ are the quark masses, and $\mathbf{p}$ is the relative momentum of the constituent quarks. In the center of mass system the relative momentum squared on the mass shell $b^2(M)$ is expressed through the meson and quark masses:

$$b^2(M)=\frac{[M^2-(m_1+m_2)^2][M^2-(m_1-m_2)^2]}{4M^2}. \tag{3}$$

It is assumed that the kernel of this equation – the interquark quasipotential $V(\mathbf{p},\mathbf{q};M)$ – consists of the perturbative one-gluon exchange (OGE) and the nonperturbative confining parts [11]

$$V(\mathbf{p},\mathbf{q};M)=\bar u_1(p)\bar v_2(-p)\mathcal{V}(\mathbf{p},\mathbf{q};M)u_1(q)v_2(-q), \tag{4}$$

with

$$\mathcal{V}(\mathbf{p},\mathbf{q};M)=\mathcal{V}(\mathbf{k})=\frac{4}{3}\alpha_s D_{\mu\nu}(\mathbf{k})\gamma_1^\mu\gamma_2^\nu+V_{\rm conf}^V(\mathbf{k})\Gamma_1^\mu(\mathbf{k})\Gamma_{2;\mu}(\mathbf{k})+V_{\rm conf}^S(\mathbf{k}),$$

where $\mathbf{k}=\mathbf{p}-\mathbf{q}$, α_s is the QCD coupling constant, $D_{\mu\nu}$ is the gluon propagator in the Coulomb gauge, while γ_μ and u_1, v_2 are the Dirac matrices and spinors, respectively.

The confining part is taken as the mixture of the Lorentz-scalar and Lorentz-vector linearly rising interactions which in the nonrelativistic limit reduce to

$$V_{\rm conf}(r)=V_{\rm conf}^S(r)+V_{\rm conf}^V(r)=Ar+B, \tag{5}$$

with

$$V_{\rm conf}^V(r)=(1-\varepsilon)(Ar+B),\qquad V_{\rm conf}^S(r)=\varepsilon(Ar+B). \tag{6}$$

Therefore, in this limit the Cornell-type potential is reproduced

$$V_{\rm NR}(r)=-\frac{4}{3}\frac{\alpha_s}{r}+Ar+B.$$

The value of the mixing coefficient $\varepsilon=-1$ has been obtained from the consideration of the heavy quark expansion for the semileptonic $B\to D^{(*)}$ decays [12] and charmonium radiative decays [11].

For the QCD coupling constant $\alpha_s\equiv\alpha_s(\mu^2)$ we set the scale $\mu=2m_1m_2/(m_1+m_2)$ and use the model with freezing [13]

$$\alpha_s(\mu^2)=\frac{4\pi}{\beta_0\ln\dfrac{\mu^2+M_B^2}{\Lambda^2}},\qquad \beta_0=11-\frac{2}{3}n_f, \tag{7}$$

where the background mass is $M_B=2.24\sqrt{A}=0.95$ GeV, and $\Lambda=413$ MeV was fixed in our model from fitting light and heavy-light meson spectra [11].

The vector vertex of the confining interaction contains the additional Pauli term with the nonperturbative anomalous chromomagnetic moment of the quark κ

$$\Gamma_\mu(\mathbf{k})=\gamma_\mu+\frac{i\kappa}{2m}\sigma_{\mu\nu}k^\nu. \tag{8}$$

We fixed the value $\kappa=-1$ by analyzing the fine splittings of heavy quarkonia ^3P_J-states [11] and the heavy quark expansion for semileptonic decays of heavy mesons [12] and baryons [14]. It enables the vanishing of the spin-dependent chromomagnetic interaction, proportional to $(1+\kappa)$, in accord with the flux tube model. The constituent quark masses $m_b=4.88$ GeV, $m_c=1.55$ GeV, $m_s=0.5$ GeV, $m_{u,d}=0.33$ GeV and the parameters of

the linear potential $A = 0.18$ GeV^2 and $B = -0.30$ GeV were determined from the previous analysis of meson spectroscopy [11]. Note that we have used a universal set of model parameters for the calculations of the meson, baryon and tetraquark spectra as well as their weak and radiative decays.

In the following section we apply our relativistic quark model to the consideration of the strong decays of vector mesons to a pair of pseudoscalar mesons.

3. Relativistic description of strong decays in a microscopic decay model

The current–current interaction in the microscopic decay model [9] is described by the following Hamiltonian

$$H_I = \frac{1}{2}\int\int d^3x d^3y\, J(\mathbf{x})\frac{\lambda^a}{2}V(|\mathbf{x}-\mathbf{y}|)J(\mathbf{y})\frac{\lambda^a}{2}, \tag{9}$$

where in our model the quark current J is given by

$$J \equiv \bar\psi\Gamma\psi = \begin{cases} \bar\psi\psi \quad \text{scalar confining interaction,} \\ \bar\psi(\gamma^\mu + i\frac{\kappa}{2m}\sigma^{\mu\nu}k_\nu)\psi \\ \quad \text{vector confining interaction with the Pauli term,} \\ \bar\psi\gamma^0\psi \quad \text{color Coulomb OGE,} \\ (\bar\psi\gamma^i\psi)_T \quad \text{transverse OGE,} \end{cases} \tag{10}$$

and the interaction kernel V, according to Ref. [9], is defined as

$$V(r) = \begin{cases} \frac{3}{4}\varepsilon(Ar+B) & \text{scalar confining interaction,} \\ \frac{3}{4}(1-\varepsilon)(Ar+B) & \text{vector confining interaction,} \\ \alpha_s/r & \text{color Coulomb OGE,} \\ -\alpha_s/r & \text{transverse OGE.} \end{cases} \tag{11}$$

Here the confinement kernel is normalized so that one gets the confining potentials in Eq. (5) of a color-singlet $q\bar q$ pair.

The strong decay process $A \to BC$, where mesons have the following quark content: $A(Q\bar Q')$, $B(Q\bar q)$, $C(q\bar Q')$, is described by the two diagrams given in Fig. 1. The corresponding decay matrix element can be presented as

$$\langle BC|H_I|A\rangle = h_{fi}\,\delta(\mathbf{P}_A - \mathbf{P}_B - \mathbf{P}_C), \tag{12}$$

where $\mathbf{P}_I$ $(I = A, B, C)$ are three-momenta of mesons and the δ-function accounts for the momentum conservation. The matrix element h_{fi} is the product of the Fermi signature phase (due to permutation of quark and antiquark operators) $I_{\text{signature}}$ and the color I_{color}, flavor I_{flavor} and spin-space $I_{\text{spin-space}}$ factors

$$h_{fi} = I_{\text{signature}}\, I_{\text{color}}\, I_{\text{flavor}}\, I_{\text{spin-space}}. \tag{13}$$

The expressions for the factors $I_{\text{signature}}$, I_{color} and I_{flavor} can be found in Ref. [9].

The spin-space factor $I_{\text{spin-space}}$ can be expressed through the overlap integral of the meson wave functions. In the rest frame of the decaying meson A ($\mathbf{P}_A = 0$, $\mathbf{P}_B = -\mathbf{P}_C = \mathbf{\Delta}$) the contribution of the $(d1)$ diagram in Fig. 1 is given by

$$I_{\text{spin-space}}(d1) = \int\int \frac{d^3p d^3q}{(2\pi)^3}\bar\Psi_{B\,\mathbf{\Delta}}(2\mathbf{q}-\mathbf{\Delta})\bar\Psi_{C\,-\mathbf{\Delta}}(2\mathbf{p}-\mathbf{\Delta}) \times [\bar u_Q(q)\Gamma u_Q(p)] \times \mathcal{V}(\mathbf{p}-\mathbf{q})[\bar u_q(p-\Delta)\Gamma v_q(-q+\Delta)]\Psi_{A\,\mathbf{0}}(2\mathbf{p}). \tag{14}$$

It is important to note that the wave functions entering the decay matrix element (14) are not in the rest frame. In the chosen frame,

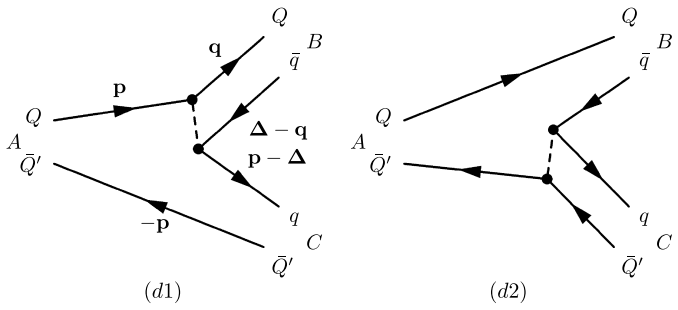

Fig. 1. Diagrams of the strong decay $A \to BC$.

where the initial vector A meson is at rest ($\mathbf{P}_A = 0$), the final B and C mesons are moving with the recoil momenta $\mathbf{P}_B = -\mathbf{P}_C = \mathbf{\Delta}$. The wave function of the moving $M(q_1\bar q_2)$ meson $\Psi_{M\,\mathbf{\Delta}}$ is connected with the wave function in the rest frame $\Psi_{M\,\mathbf{0}} \equiv \Psi_M$ by the transformation [15]

$$\Psi_{M\,\mathbf{\Delta}}(\mathbf{p}) = D^{1/2}_{q_1}(R^W_{L_\mathbf{\Delta}})D^{1/2}_{q_2}(R^W_{L_\mathbf{\Delta}})\Psi_{M\,\mathbf{0}}(\mathbf{p}), \tag{15}$$

where q_1, q_2 denote $Q\,(Q')$ or q; R^W is the Wigner rotation, $L_\mathbf{\Delta}$ is the Lorentz boost from the meson rest frame to a moving one, and the rotation matrix $D^{1/2}(R)$ in spinor representation is given by

$$\begin{pmatrix} 1 & 0 \\ 0 & 1 \end{pmatrix} D^{1/2}_{q_i}(R^W_{L_\mathbf{\Delta}}) = S^{-1}(\mathbf{p}_{q_i})S(\mathbf{\Delta})S(\mathbf{p}), \qquad (i = 1, 2), \tag{16}$$

where

$$S(\mathbf{p}) = \sqrt{\frac{\epsilon(p)+m}{2m}}\left(1 + \frac{\boldsymbol{\alpha}\mathbf{p}}{\epsilon(p)+m}\right)$$

is the usual Lorentz transformation matrix of the four-spinor and $\epsilon(p) = \sqrt{m^2+\mathbf{p}^2}$ is the quark energy.

Substituting corresponding spinors in Eq. (14) and taking into account the wave function transformations (15) and spin structure of the initial vector $(^3S_1)$ and final pseudoscalar $(^1S_0)$ mesons, we get the spin-space factor in the form

$$I_{\text{spin-space}}(d1) = \int\int \frac{d^3p d^3q}{(2\pi)^3}\bar\Psi_{B,\mathbf{0}}(2\mathbf{q}-\mathbf{\Delta})\bar\Psi_{C,\mathbf{0}}(2\mathbf{p}-\mathbf{\Delta}) \times \mathcal{M}(\mathbf{p},\mathbf{q})\mathcal{V}(\mathbf{p}-\mathbf{q})\Psi_{A,\mathbf{0}}(2\mathbf{p}), \tag{17}$$

with the functions $\mathcal{M}(\mathbf{p},\mathbf{q})$ given by the following expressions.

(a) Scalar confining interaction $\Gamma = I$

$$\begin{aligned} &\mathcal{M}_{\text{scal}}(\mathbf{p},\mathbf{q}) \\ &= \sqrt{\frac{\epsilon_Q(q)+m_Q}{2\epsilon_Q(q)}}\sqrt{\frac{\epsilon_Q(p)+m_Q}{2\epsilon_Q(p)}}\sqrt{\frac{\epsilon_q(p-\Delta)+m_q}{2\epsilon_q(p-\Delta)}} \\ &\times\sqrt{\frac{\epsilon_q(q-\Delta)+m_q}{2\epsilon_q(q-\Delta)}} \\ &\times\Bigg[p_+\Bigg\{-\frac{1}{\epsilon_q(p-\Delta)+m_q} \\ &\times\left(1-\frac{1}{2}\frac{\mathbf{\Delta}^2-(E_B-M_B)(E_C-M_C)}{(E_C+M_C)(\epsilon_{\bar Q'}(p-\Delta)+m_{\bar Q'})}\right) \\ &+\frac{1}{2}\frac{\mathbf{\Delta}^2+(E_B+M_B)(E_C-M_C)}{(E_C+M_C)(\epsilon_{\bar Q'}(p-\Delta)+m_{\bar Q'})(\epsilon_q(q-\Delta)+m_q)}\Bigg\} \\ &+q_+\Bigg\{-\frac{1}{\epsilon_q(q-\Delta)+m_q} \end{aligned}$$

$$\times\left(1-\frac{1}{2}\frac{\mathbf{\Delta}^2+(E_B+M_B)(E_C-M_C)}{(E_B+M_B)(\epsilon_Q(q-\Delta)+m_Q)}\right)$$
$$+\frac{1}{2}\frac{\mathbf{\Delta}^2-(E_B-M_B)(E_C-M_C)}{(E_B+M_B)(\epsilon_Q(q-\Delta)+m_Q)(\epsilon_q(p-\Delta)+m_q)}\Bigg\}\Bigg], \tag{18}$$

(b) vector confining interaction with the Pauli term $\Gamma=\gamma^\mu+i\frac{\kappa}{2m}\sigma^{\mu\nu}k_\nu$ for $\kappa=-1$

$$\mathcal{M}_{\rm vect}(\mathbf{p},\mathbf{q})$$
$$=\sqrt{\frac{\epsilon_Q(q)+m_Q}{2\epsilon_Q(q)}}\sqrt{\frac{\epsilon_Q(p)+m_Q}{2\epsilon_Q(p)}}\sqrt{\frac{\epsilon_q(p-\Delta)+m_q}{2\epsilon_q(p-\Delta)}}$$
$$\times\sqrt{\frac{\epsilon_q(q-\Delta)+m_q}{2\epsilon_q(q-\Delta)}}$$
$$\times\Bigg[p_+\Bigg\{-\frac{1}{\epsilon_Q(p-\Delta)+m_Q}$$
$$\times\left(1-\frac{M_B(E_C-M_C)}{(E_C+M_C)(\epsilon_{\bar{Q}'}(p-\Delta)+m_{\bar{Q}'})}\right)\Bigg\}$$
$$+q_+\Bigg\{-\frac{1}{\epsilon_Q(q-\Delta)+m_Q}$$
$$\times\left(1-\frac{M_B(E_C-M_C)}{(E_B+M_B)(\epsilon_Q(q-\Delta)+m_Q)}\right)\Bigg\}\Bigg], \tag{19}$$

(c) color Coulomb OGE $\Gamma=\gamma^0$

$$\mathcal{M}_{\rm Coul}(\mathbf{p},\mathbf{q})$$
$$=\sqrt{\frac{\epsilon_Q(q)+m_Q}{2\epsilon_Q(q)}}\sqrt{\frac{\epsilon_Q(p)+m_Q}{2\epsilon_Q(p)}}\sqrt{\frac{\epsilon_q(p-\Delta)+m_q}{2\epsilon_q(p-\Delta)}}$$
$$\times\sqrt{\frac{\epsilon_q(q-\Delta)+m_q}{2\epsilon_q(q-\Delta)}}$$
$$\times\Bigg[p_+\Bigg\{\frac{1}{\epsilon_q(p-\Delta)+m_q}$$
$$\times\left(1-\frac{1}{2}\frac{\mathbf{\Delta}^2-(E_B-M_B)(E_C-M_C)}{(E_C+M_C)(\epsilon_{\bar{Q}'}(p-\Delta)+m_{\bar{Q}'})}\right)$$
$$-\frac{1}{2}\frac{\mathbf{\Delta}^2+(E_B+M_B)(E_C-M_C)}{(E_C+M_C)(\epsilon_{\bar{Q}'}(p-\Delta)+m_{\bar{Q}'})(\epsilon_q(q-\Delta)+m_q)}\Bigg\}$$
$$+q_+\Bigg\{-\frac{1}{\epsilon_q(q-\Delta)+m_q}$$
$$\times\left(1-\frac{1}{2}\frac{\mathbf{\Delta}^2+(E_B+M_B)(E_C-M_C)}{(E_B+M_B)(\epsilon_Q(q-\Delta)+m_Q)}\right)$$
$$+\frac{1}{2}\frac{\mathbf{\Delta}^2-(E_B-M_B)(E_C-M_C)}{(E_B+M_B)(\epsilon_Q(q-\Delta)+m_Q)(\epsilon_q(p-\Delta)+m_q)}\Bigg\}\Bigg], \tag{20}$$

(d) transverse OGE $\Gamma=\gamma_T^i$

$$\mathcal{M}_T(\mathbf{p},\mathbf{q})$$
$$=\sqrt{\frac{\epsilon_Q(q)+m_Q}{2\epsilon_Q(q)}}\sqrt{\frac{\epsilon_Q(p)+m_Q}{2\epsilon_Q(p)}}\sqrt{\frac{\epsilon_q(p-\Delta)+m_q}{2\epsilon_q(p-\Delta)}}$$
$$\times\sqrt{\frac{\epsilon_q(q-\Delta)+m_q}{2\epsilon_q(q-\Delta)}}$$
$$\times\Bigg[p_+\Bigg\{\frac{1}{\epsilon_Q(p-\Delta)+m_Q}$$
$$\times\left(1+\frac{1}{2}\frac{\mathbf{\Delta}^2+(E_B-M_B)(E_C-M_C)}{(E_C+M_C)(\epsilon_{\bar{Q}'}(p-\Delta)+m_{\bar{Q}'})}\right)$$
$$+\frac{1}{2}\frac{\mathbf{\Delta}^2-(E_B+M_B)(E_C-M_C)}{(E_C+M_C)(\epsilon_{\bar{Q}'}(p-\Delta)+m_{\bar{Q}'})(\epsilon_Q(q)+m_Q)}\Bigg\}$$
$$+q_+\Bigg\{\frac{1}{\epsilon_Q(q)+m_Q}\left(1+\frac{1}{2}\frac{\mathbf{\Delta}^2-(E_B+M_B)(E_C-M_C)}{(E_B+M_B)}\right.$$
$$\times\left.\left(\frac{1}{\epsilon_q(q)+m_q}+\frac{1}{\epsilon_Q(q-\Delta)+m_Q}\right)\right)$$
$$-\frac{1}{2}\frac{\mathbf{\Delta}^2+(E_B-M_B)(E_C-M_C)}{(E_B+M_B)(\epsilon_Q(p)+m_Q)}$$
$$\times\left(\frac{1}{\epsilon_q(q)+m_q}-\frac{1}{\epsilon_Q(q-\Delta)+m_Q}\right)\Bigg\}\Bigg]$$
$$+\frac{\mathbf{\Delta}^2+(E_B-M_B)(E_C-M_C)}{E_B^2}$$
$$\times\left(\frac{E_C+M_C}{E_B+M_B}-\frac{E_B^2}{\mathbf{\Delta}^2+(E_B+M_B)(E_C+M_C)}\right)\mathcal{M}_{\rm Coul}(\mathbf{p},\mathbf{q}), \tag{21}$$

where the p_+, q_+ momenta are given by $p_+=1/2(p_x+ip_y)=-\sqrt{\frac{2\pi}{3}}pY_{11}(\Omega)$ and $q_+=1/2(q_x+iq_y)=-\sqrt{\frac{2\pi}{3}}qY_{11}(\Omega)$, and the final meson energies are $E_I=\sqrt{M_I^2+\mathbf{\Delta}^2}$ $(I=B,C)$.

The expressions for the contribution of the $(d2)$ diagram in Fig. 1 can be obtained from Eqs. (18)–(21) by the obvious replacements $(Q\leftrightarrow Q',\ M_B\leftrightarrow M_C)$.

4. Results

The differential decay rate of the strong decay $A\to BC$ is expressed through the decay amplitude h_{fi} by [9]

$$\frac{d\Gamma_{A\to BC}}{d\Omega}=2\pi\frac{|\mathbf{\Delta}|E_BE_C}{M_A}|h_{fi}|^2, \tag{22}$$

where the modulus of the recoil momentum of the final mesons is given by

$$|\mathbf{\Delta}|=\frac{\sqrt{[M_A^2-(M_B+M_C)^2][M_A^2-(M_B-M_C)^2]}}{2M_A}.$$

Now we substitute the relativistic meson wave functions, obtained previously in the calculations of meson mass spectra [11], into Eqs. (13), (17)–(22) and determine the corresponding decay amplitudes and decay rates. The results for the strong decay rates of vector $(^3S_1)$ mesons into a pair of pseudoscalar $(^1S_0)$

Table 1
Strong decay rates of vector ($^3S_1$) mesons into a pair of pseudoscalar ($^1S_0$) mesons (in MeV).

Decay	Γ_{our}	$\Gamma_{^3P_0}$ [9,16]	$\Gamma_{^3P_0}$ [7,17]	$\Gamma_{mic.}$ [17]	Γ_{DS} [18]	Γ_{NJL} [19]	Γ_{exp} [1]
$\rho \to \pi\pi$	124	79	160		118	149	147.8 ± 0.9
$\phi \to K\bar{K}$	3.3	2.5				4.2	3.55 ± 0.05
$K^* \to K\pi$	46	21			52	51	47.4 ± 0.6
$D^* \to D\pi$	0.062	0.025	0.036		0.038	0.063	0.082 ± 0.002
$\rho(2S) \to \pi\pi$	160	74				22	
$\rho(2S) \to K\bar{K}$	14	35					
$\phi(2S) \to K\bar{K}$	17	89				10	
$D^*(2S) \to D\pi$	20	1					
$D^*(2S) \to D_sK$	2.6	0.1					
$D^*(2S) \to D\eta$	2.2	0.4					
$D_s^*(2S) \to DK$	21	17					
$D_s^*(2S) \to D_s\eta$	1.4	2.6					
$\Psi(3S) \to D\bar{D}$	11	0.1	4.61	10.17			
$\Psi(3S) \to D_s\bar{D}_s$	4.0	7.8	2.08	1.14			
$\Upsilon(4S) \to B\bar{B}$	18		20.59				20.5 ± 2.5
$\Upsilon(5S) \to B\bar{B}$	4.3						3.0 ± 1.7
$\Upsilon(5S) \to B_s\bar{B}_s$	0.3						0.28 ± 0.28

mesons are given in Table 1 in comparison with the predictions of the $^3P_0$ model [7,9,16], the microscopic model [17], the Dyson–Schwinger (DS) equation model [18], the Nambu–Jona-Lasinio (NJL) quark model [19] and available experimental data [1]. The results are presented for the decays of light (ρ, ϕ, K^*), heavy-light (D^*, D_s^*) mesons and heavy (Ψ, Υ) quarkonia. Note that in our calculations we consistently take into account the relativistic structure of the strong decay amplitudes, transformations of the meson wave functions from the rest to the moving reference frame as well as the corrections to the rest frame wave functions originating from the relativistic contributions to the quark–antiquark interaction potential, which are treated nonperturbatively in our model. We find that our predictions agree well with the available experimental data.

It is interesting to analyze the role of the relativistic contributions to the considered strong decay rates. We use the $\rho \to \pi\pi$ decay as an example since both initial and final mesons contain only light quarks and thus relativistic effects are very important. Taking the nonrelativistic limit of expressions (18)–(21) and calculating the strong decay rate (22), we get $\Gamma^{NR}(\rho \to \pi\pi) = 331$ MeV. Omitting contributions coming from the Lorentz boost of the meson wave functions in the relativistic expressions (18)–(21) we get the $\rho \to \pi\pi$ decay rate of 145 MeV, while complete relativistic calculation gives $\Gamma(\rho \to \pi\pi) = 124$ MeV. Therefore we conclude that the account of the relativistic structure of the decay amplitude reduces the nonrelativistic $\rho \to \pi\pi$ decay rate by 56%, while the relativistic transformations of the meson wave functions give additional reduction of 6.4%. We can also analyze contributions of the different Lorentz structures of the interaction potential to the decay rate. The contributions of potentials considered separately are the following. The scalar confining interaction: $\Gamma^S(\rho \to \pi\pi) = 54$ MeV; the vector confining interaction: $\Gamma^V(\rho \to \pi\pi) = 106$ MeV; the one-gluon exchange (OGE): $\Gamma^{OGE}(\rho \to \pi\pi) = 4.4$ MeV.

In principle, the similar analysis can be done for other considered decays. Here we additionally present results for the $\Psi(3S) \to D\bar{D}$ decay, since it involves both light (u, d) and heavy (c) quarks. In the nonrelativistic limit we get $\Gamma^{NR}(\Psi(3S) \to D\bar{D}) = 18.6$ MeV. Account of the relativistic structure of the decay amplitude reduces it by 38%, while the relativistic transformations of the meson wave functions give additional reduction of 2.7%, leading to the final value $\Gamma(\Psi(3S) \to D\bar{D}) = 11$ MeV. The contributions of the Lorentz structures of the interaction potential are now the following: $\Gamma^S(\Psi(3S) \to D\bar{D}) = 32$ MeV; $\Gamma^V(\Psi(3S) \to D\bar{D}) = 18$ MeV; $\Gamma^{OGE}(\Psi(3S) \to D\bar{D}) = 0.23$ MeV. We see that, as naively expected, the role of the relativistic effects is somewhat reduced for the strong decays of heavy mesons, especially the ones coming from the recoil of final mesons (15).

The results of Refs. [9,16] are based on the $^3P_0$ model with the universal flavor independent strength parameter γ, while in Refs. [7,17] the authors take into account the scaling of γ with the reduced mass of the quark–antiquark pair in the decaying meson. The account for such scaling, which was found to be logarithmic in the reduced mass, improves agreement of the predictions with experimental data, but introduces an additional free parameter, which determines the scaling. In all these calculations Gaussian wave functions were used.

The main advantage of the microscopic approach consists in the fact that it completely determines the strong decay dynamics without introducing a strength parameter responsible for the production of the light quark pair. In Ref. [9] the microscopic model was used for the decay rate of the ρ meson with the result $\Gamma_{\rho\to\pi\pi} = 243$ MeV, which is too large relative to data. The possible sources of this overestimate were attributed to the nonrelativistic consideration and the choice of the $q\bar{q}$ wave functions in a simple harmonic oscillator form. Our calculations confirm this conjecture. As a result, the prediction for the $\rho \to \pi\pi$ decay rate is reduced by almost a factor of two in fair agreement with data. In Ref. [17] the microscopic model was applied to strong charmonium decays. The employed model uses for the quark–antiquark interaction the sum of one-gluon exchange, a nonperturbative confining term with scalar/vector Lorentz structure including phenomenological string-breaking effects and (in case of light mesons) Goldstone-boson exchange potentials. Calculations of the strong decays were carried out in the nonrelativistic limit. We find that our relativistic prediction for the $\Psi(3S) \to D\bar{D}$ decay rate agree well with the result of Ref. [17], while the one for the $\Psi(3S) \to D_s\bar{D}_s$ decay rate differ by almost a factor of four. The possible origin of this discrepancy can be attributed to the difference in the wave functions and to the treatment of the relativistic effects. As it was noted in Ref. [20], this decay should be very sensitive to the position of nodes of the $\Psi(3S)$ wave function and the resulting nodes in the decay amplitude.

We find a reasonable agreement of our results with the predictions of the relativistic quark model based on the DS equation [18] and the NJL model [19]. The only exception is the significant difference of our and the NJL model [19] values for the $\rho(2S) \to \pi\pi$ decay. Note that the $^3P_0$ model [16] gives the intermediate result. Therefore experimental measurement of this decay rate can help to discriminate theoretical approaches.

Strong decays of the D^* mesons deserve a special attention, since the phase space for their decays to the D meson and π is

Table 2
Decay rates and branching fractions of the D^* mesons.

Decay	Γ (keV)		Br			
	our	Experiment [1]	our	DS [18]	QCM [22]	Experiment [1]
$D^*(2010)^+ \to D^0\pi^+$	42	56 ± 1.5	0.667	0.683	0.687	0.677 ± 0.005
$\to D^+\pi^0$	20	25.6 ± 0.9	0.317	0.316	0.309	0.307 ± 0.005
$\to D^+\gamma$	1.04	1.3 ± 0.5	0.016	0.001	0.004	0.016 ± 0.004
Total	63	83.4 ± 1.8				
$D^*(2007)^0 \to D^0\pi^0$	19		0.623	0.826	0.682	0.619 ± 0.029
$\to D^0\gamma$	11.5		0.377	0.174	0.318	0.381 ± 0.029
Total	30.5	<2100				

small. Indeed, decays of the charged $D^*(2010)^+$ meson are kinematically allowed both to $D^0\pi^+$ and $D^+\pi^0$, while the neutral $D^*(2007)^0$ meson can strongly decay only to $D^0\pi^0$. Due to the strong phase space suppression of strong decays of the D^* mesons, their radiative decays start to play an important role. Such radiative decays were calculated in our paper [21] with the comprehensive account of relativistic effects. In Table 2 we confront our predictions for the decay rates and branching fractions of the charged and neutral D^* mesons with previous calculations based on the DS equation [18] and the relativistic confinement quark model (QCM) [22] and available experimental data. Good agreement of theoretical results and data is observed. Note that in Ref. [23] the strong decay of the charged D^{*+} meson to neutral D^0 meson and pion was considered in the quark model which incorporates heavy quark symmetry and chiral dynamics. The prediction for the decay rate $\Gamma(D^{*+} \to D^0\pi^+) = 100$ keV (for the favored value of the constant f) was obtained which is somewhat larger than the measured rate.

5. Conclusions

In this paper we propose the relativistic extension of the microscopic model of strong meson decays. It is developed in the framework of the relativistic quark model based on the quasipotential approach and QCD-motivated interquark potential. This model was previously successfully applied to the calculation of hadron spectroscopy and radiative and weak decays. Such approach allowed us to get the wave functions of light and heavy mesons with the nonperturbative account of the relativistic effects. The consistent relativistic approach for the calculation of the decay matrix elements is now applied for the calculation of the strong decay amplitudes. The relativistic transformation of meson wave functions from rest to moving reference frames is explicitly taken into account. The obtained decay matrix elements are treated without application of the nonrelativistic expansion. Here we test our approach in calculating strong decays of the vector ($^3S_1$) mesons to the pair of pseudoscalar ($^1S_0$) mesons. The presence of only S-wave mesons in the initial and final states significantly simplifies the angular integration in the decay matrix elements. The decay rates are obtained for decays of light, heavy-light mesons and heavy quarkonia. All calculations are performed with all model parameters kept fixed from previous calculations of meson spectroscopy. No additional parameters are necessary for describing the production of the light $q\bar{q}$ pair, since it is considered to originate from the same interaction term as the interquark potential. The obtained results are confronted with calculations within the $^3P_0$ model, the DS equation model, the NJL model and nonrelativistic microscopic models as well as available experimental data. The overall agreement of the obtained results with experiment is found.

Acknowledgements

The authors are grateful to M.A. Ivanov, V.A. Matveev, D.I. Melikhov and V.I. Savrin for useful discussions. This work was supported in part by the *Russian Foundation for Basic Research* under Grant No. 12-02-00053-a.

References

[1] K.A. Olive, et al., Particle Data Group, Chin. Phys. C 38 (2014) 090001.
[2] N. Brambilla, et al., Eur. Phys. J. C 71 (2011) 1534.
[3] D. Ebert, H. Reinhardt, M.K. Volkov, Prog. Part. Nucl. Phys. 33 (1994) 1.
[4] J.W. Alcock, M.J. Burfitt, W.N. Cottingham, Z. Phys. C 25 (1984) 161;
S. Kumano, V.R. Pandharipande, Phys. Rev. D 38 (1988) 146.
[5] P. Geiger, E.S. Swanson, Phys. Rev. D 50 (1994) 6855.
[6] L. Micu, Nucl. Phys. B 10 (1969) 521;
A. Le Yaouanc, L. Oliver, O. Pene, J.C. Raynal, Phys. Rev. D 8 (1973) 2223;
T. Barnes, F.E. Close, P.R. Page, E.S. Swanson, Phys. Rev. D 55 (1997) 4157.
[7] J. Segovia, D.R. Entem, F. Fernandez, Phys. Lett. B 715 (2012) 322.
[8] N. Isgur, J.E. Paton, Phys. Rev. D 31 (1985) 2910;
R. Kokoski, N. Isgur, Phys. Rev. D 35 (1987) 907.
[9] E.S. Ackleh, T. Barnes, E.S. Swanson, Phys. Rev. D 54 (1996) 6811.
[10] Y.A. Simonov, Phys. Rev. D 84 (2011) 065013.
[11] D. Ebert, R.N. Faustov, V.O. Galkin, Phys. Rev. D 67 (2003) 014027;
D. Ebert, R.N. Faustov, V.O. Galkin, Phys. Rev. D 79 (2009) 114029;
D. Ebert, R.N. Faustov, V.O. Galkin, Eur. Phys. J. C 66 (2010) 197;
D. Ebert, R.N. Faustov, V.O. Galkin, Phys. Rev. D 84 (2011) 014025;
D. Ebert, R.N. Faustov, V.O. Galkin, Eur. Phys. J. C 71 (2011) 1825.
[12] R.N. Faustov, V.O. Galkin, Z. Phys. C 66 (1995) 119.
[13] A.M. Badalian, A.I. Veselov, B.L.G. Bakker, Phys. Rev. D 70 (2004) 016007;
Yu.A. Simonov, Phys. At. Nucl. 58 (1995) 107.
[14] D. Ebert, R.N. Faustov, V.O. Galkin, Phys. Rev. D 73 (2006) 094002.
[15] R.N. Faustov, Ann. Phys. 78 (1973) 176;
R.N. Faustov, Nuovo Cimento A 69 (1970) 37.
[16] T. Barnes, F.E. Close, P.R. Page, E.S. Swanson, Phys. Rev. D 55 (1997) 4157;
T. Barnes, N. Black, P.R. Page, Phys. Rev. D 68 (2003) 054014;
F.E. Close, E.S. Swanson, Phys. Rev. D 72 (2005) 094004;
T. Barnes, S. Godfrey, E.S. Swanson, Phys. Rev. D 72 (2005) 054026.
[17] J. Segovia, D.R. Entem, F. Fernandez, Nucl. Phys. A 915 (2013) 125.
[18] M.A. Ivanov, Y.L. Kalinovsky, C.D. Roberts, Phys. Rev. D 60 (1999) 034018.
[19] M.P. Khanna, M.K. Volkov, Theor. Math. Phys. 102 (1995) 158;
M.P. Khanna, M.K. Volkov, Teor. Mat. Fiz. 102 (1995) 217;
M.K. Volkov, D. Ebert, M. Nagy, Int. J. Mod. Phys. A 13 (1998) 5443;
M.K. Volkov, V.L. Yudichev, D. Ebert, J. Phys. G 25 (1999) 2025.
[20] A. Le Yaouanc, L. Oliver, O. Pene, J.-C. Raynal, Phys. Lett. B 71 (1977) 397.
[21] D. Ebert, R.N. Faustov, V.O. Galkin, Phys. Lett. B 537 (2002) 241.
[22] M.A. Ivanov, Y.M. Valit, Z. Phys. C 67 (1995) 633.
[23] T.M. Yan, H.Y. Cheng, C.Y. Cheung, G.L. Lin, Y.C. Lin, H.L. Yu, Phys. Rev. D 46 (1992) 1148;
T.M. Yan, H.Y. Cheng, C.Y. Cheung, G.L. Lin, Y.C. Lin, H.L. Yu, Phys. Rev. D 55 (1997) 5851 (Erratum).